IEEE Access
Multidisciplinary ⋮ Rapid Review ⋮ Open Access Journal

Received May 6, 2020, accepted May 12, 2020, date of publication May 25, 2020, date of current version June 8, 2020.

Digital Object Identifier 10.1109/ACCESS.2020.2997002

Load Frequency Stability Analysis of Time-Delayed Multi-Area Power Systems With EV Aggregators Based on Bessel-Legendre Inequality and Model Reconstruction Technique

SHA-JUN ZHOU, HONG-BING ZENG, AND HUI-QIN XIAO
School of Electrical and Information Engineering, Hunan University of Technology, Zhuzhou 412007, China

Corresponding authors: Hong-Bing Zeng (9804zhb@163.com) and Hui-Qin Xiao (xiaohq_610@126.com)

This work was supported in part by the National Natural Science Foundation of China under Grant 61703153, and in part by the Natural Science Foundation of Hunan Province under Grant 2018JJ2096 and Grant 2018JJ4075.

ABSTRACT This paper investigates the stability of time-delayed load frequency control (LFC) systems with electric vehicles (EV) aggregators based on Lyapunov theory and linear matrix inequality (LMI) technology. A novel Lyapunov-Krasovskii functional (LKF) is constructed. Then, based on Bessel-Legendre (B-L) inequality and model reconstruction technique, two stability criteria are derived, respectively. Some simulations are carried out to verify the effectiveness of the proposed methods. And the interaction of time-delays between areas and the effect of gains of EVs on delay margins are discussed.

INDEX TERMS Electric vehicles, load frequency control, Bessel-Legendre inequality, model reconstruction technique.

I. INTRODUCTION

Whether it is the traditional power system under the vertical integration mode, or deregulated power system composed of different market players, the stability of load frequency is one of the most important indexes to measure the normal operation of the power grid [1]. For interconnected power systems, LFC is the most commonly used approach to keep the load frequency stable or changing at a small range. Besides, it can also regulate the tie-line powers exchanges within a desired value [2].

Nowadays, with the increasingly serious energy crisis, new energy has been vigorously developed to improve the structure of energy. As EVs becoming power sources relying on electric energy, and the EV's power storage battery technology growing maturity, the number of EVs will continue to increase [3]. EV will bring a huge development potential for power grid because of its less contamination, the ability to improve energy consumption structure and the characteristic for energy saving. Certainly, with those social advantages and environmental benefits, considerable public attention has been paid to the development of EVs. Under the concept of V2G, EVs are not only the users of power grid, but also the participants maintaining the stability of power grid, which realizes the two-way interaction between energy storage system and power grid. By V2G technology, EV can play roles of peak shaving and valley filling for the load of power grid. In addition, EVs can be participants of LFC [4]. As a kind of mobile energy storage equipment, EVs can control the balance of supply and demand by controlling the charge and discharge of electricity. Due to this, EVs are able to control the system frequency fluctuation caused by load disturbance rapidly [5].

Communication networks have been applied to LFC systems for many years to transmit control signals. The existence of time-delays is inevitable because of the network bandwidth capacity. These time-delays may deteriorate the performance of power systems like instability or oscillation, or at least, cause the load frequency to deviate from the desired value [6], [7]. With regard to stability research of time-delay systems, there are two main methods [8]. One is frequency domain method which can obtain the sufficient and necessary conditions for the system stability but it can only deal with systems with constant time-delays. Another method most commonly used now is the time domain indirect method based on LKF and LMI

The associate editor coordinating the review of this manuscript and approving it for publication was Xiaosong Hu.

technology. This method can only obtain the sufficient conditions for the system stability, so how to reduce the conservativeness has become a hot topic recently [9]–[12]. Thus, numerous inequalities have been proposed in the recent years such as Jensen inequality, Wirtinger inequality [13], Free-matrix-based inequality [14], [15], B-L inequality [26] and so on. These methods are widely used in stability analysis of time-delayed LFC systems and have achieved remarkable results. Jensen inequality was applied to stability analysis of time-delayed multi-area LFC systems [16], while Wirtinger inequality reduced the conservativeness and gave a more accurate delay margin than Jensen inequality [17]. In [18], a new auxiliary-function-based double integral inequality is proposed for stability analysis of one-area and multi-area LFC systems with time-varying delays. In [19], a delay-dependent robust controller is designed for multi-area LFC systems.

As to the time-delayed power system with EV aggregators, there are not many researches for it. In [20], a stability analysis for the time-delayed LFC system with EV aggregators is presented, where the detailed relationship between PI controller gains and delay margins is provided. In [21], a parameter uncertain model is proposed and the corresponding delay-dependent controller is designed. In addition, a novel distributed control strategy of high voltage direct current links for time-delayed LFC systems with EVs is presented in [22], which reduces the differences in frequencies between the connected power areas. In [23], a reference model of EVs' battery system and functions which describe battery state of EVs are presented. However, there are few researches considering the interrelation and interaction of time-delays between areas. Furthermore, how to obtain more accurate delay margins with less computational complex is still a difficult problem.

This paper gives a load frequency stability analysis of time-delayed multi-area power systems with EV aggregators based on B-L inequality and model reconstruction technique. The main purpose of this paper is to achieve more accurate delay margins of time-delayed multi-area LFC systems with EV aggregators. The main contents and contributions of this paper are as follows: Firstly, a novel LFK based on B-L inequality for stability analysis of LFC systems with EV aggregators is established. Secondly, an improved criterion is given based on model reconstruction technique that helps a lot to reduce the computational complexity. Thirdly, some case studies are presented including effectiveness of the proposed method, relationship between gains of EVs and delay margins, interaction of time-delays between two areas, and the compare of the two proposed criteria.

The remaining of this paper is organized as follows. In Section II, a dynamic model of time-delayed LFC system with EV aggregators is presented. In Section III, two improved criteria are proposed based on B-L inequality and model reconstruction technique, respectively. Section IV gives some case studies based on the presented model and Section V concludes this paper.

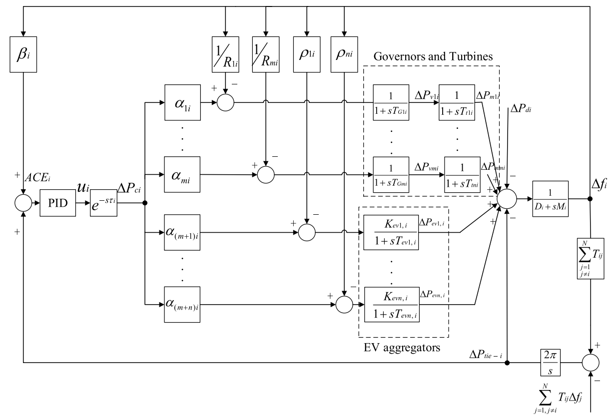

FIGURE 1. *i*-th area of time-delayed LFC system with EV aggregators.

II. MODEL OF TIME-DELAYED LFC SYSTEM WITH EV AGGREGATORS

Different from the traditional time-delayed power systems [24], EVs participating in LFC in time-delayed power system with EV aggregators. We consider N areas time-delayed LFC systems, and each one consists of m governors and turbines and n EVs. Fig. 1 describes the i-th area of time-delayed LFC system with EV aggregators. $e^{-s\tau_i}$ describes the time-delay of signal transmission. Δf_i, ΔP_{tie-i}, ΔP_{mmi}, ΔP_{vmi} are the deviation of frequency, tie-line power exchange, mechanical output of generator, and valve position, respectively; M_i, D_i, T_{Gmi}, T_{tmi}, R_{mi} denote the inertia constant, load damping coefficient, speed governor constants, turbine time constants and governor droop characteristic, respectively; β_i, α_{mi}, $\alpha_{(m+n)i}$ denote the frequency bias constant, participation ratio of governors and turbines, participation ratio of EV aggregators, respectively. The dynamic model of an EV battery system is described by [20]:

$$G_{evn,i}(s) = \frac{K_{evn,i}}{1 + T_{evn,i}} \tag{1}$$

where $K_{evn,i}$ and $T_{evn,i}$ denote the gain and time constant of the EV, respectively; ρ_{ni} and $\Delta P_{evn,i}$ are the EV droop characteristic and the deviation of power output in the EV, respectively. ACE_i is the control error of the i-th area and usually described as:

$$ACE_i = \beta_i \Delta f_i + \Delta P_{tie-i} \tag{2}$$

and a PID-type LFC controller is designed as follows:

$$u_i(t) = -K_{pi}ACE_i - K_{Ii}\int ACE_i - K_{Di}\frac{dACE_i}{dt} \tag{3}$$

Then, the closed-loop model of the time-delayed LFC system with EV aggregators can be expressed as:

$$\dot{x}(t) = Ax(t) + \sum_{i=1}^{N} A_{di}(t-\tau_i) + B_w\omega \tag{4}$$

where

$$x = [\bar{x}_1^T, \bar{x}_2^T, \ldots, \bar{x}_N^T]^T, \quad \bar{x}_i = [\hat{x}_i^T, \int y_i^T]^T, \; y_i = ACE_i$$

$$\hat{x}_i = [\Delta f_i, \Delta P_{tie-i}, \Delta P_{m1i}, \ldots, \Delta P_{mmi}, \ldots, \Delta P_{v1i}, \ldots, \Delta P_{ev1,i}, \ldots, \Delta P_{evn,i}]^T$$

$$A = \begin{bmatrix} \bar{A}_{11} & \ldots & \bar{A}_{1N} \\ \vdots & \ddots & \vdots \\ \bar{A}_{N1} & \ldots & \bar{A}_{NN} \end{bmatrix}$$

$$A_{di} = \begin{bmatrix} & 0_{(i-1)(2m+n+3)\times N(2m+n+3)} & & \\ \bar{A}_{di1} & \bar{A}_{di2} & \ldots & \bar{A}_{diN} \\ & 0_{(N\text{-i})(2m+n+3)\times N(2m+n+3)} & & \end{bmatrix}$$

$$B_w = diag\left\{\bar{B}_{w1}, \quad \bar{B}_{w2}, \quad \ldots, \quad \bar{B}_{wN}\right\}$$

$$\omega = diag\left\{\omega_1, \; \omega_2, \; \ldots, \; \omega_N\right\}$$

$$\bar{A}_{dii} = -\bar{B}_i K_i \bar{C}_i, \bar{A}_{dij} = -\bar{B}_i K_i \bar{C}_{ij}, \bar{B}_{wi} = \bar{F}_i - \bar{B}_i K_i \bar{D}_i$$

$$\bar{A}_{ii} = \begin{bmatrix} A_i & 0_{(2m+n+2)\times 1} \\ C_i & 0 \end{bmatrix}$$

$$\bar{A}_{ij} = \begin{bmatrix} A_{ij} & 0_{(2m+n+2)\times 1} \\ 0_{1\times(2m+n+2)} & 0 \end{bmatrix}$$

$$\bar{B}_i = \begin{bmatrix} B_i \\ 0 \end{bmatrix}, \; \bar{F}_i = \begin{bmatrix} F_i \\ 0 \end{bmatrix}, \; \bar{C}_i = \begin{bmatrix} C_i & 0 \\ 0_{1\times(2m+n+2)} & 1 \\ C_i A_{ij} & 0 \end{bmatrix}$$

$$\bar{C}_{ij} = \begin{bmatrix} 0_{1\times(2m+n+2)} & 0 \\ 0_{1\times(2m+n+2)} & 0 \\ C_i A_{ij} & 0_{(2m+n+2)\times 1} \end{bmatrix}, \quad \bar{D}_i = \begin{bmatrix} D_i \\ 0 \\ C_i F_i \end{bmatrix}$$

$$A_i = \begin{bmatrix} A_{11i} & A_{12i} & A_{13i} & A_{14i} \\ A_{21i} & A_{22i} & A_{23i} & A_{24i} \\ A_{31i} & A_{32i} & A_{33i} & A_{34i} \\ A_{41i} & A_{42i} & A_{43i} & A_{44i} \end{bmatrix}$$

$$A_{ij} = \begin{bmatrix} 0 & 0 & 0_{1\times(2m+n)} \\ -2\pi T_{ij} & 0 & 0_{1\times(2m+n)} \\ 0_{(2m+n)\times 1} & 0_{(2m+n)\times 1} & 0_{(2m+n)\times(2m+n)} \end{bmatrix}$$

$$A_{11i} = \begin{bmatrix} -\frac{D_i}{M_i} & -\frac{1}{M_i} \\ 2\pi \sum_{j=1, j\neq i}^{N} T_{ij} & 0 \end{bmatrix}$$

$$A_{12i} = \begin{bmatrix} \frac{1}{M_i} & \cdots & \frac{1}{M_i} \\ & 0_{1\times m} & \end{bmatrix}, \quad A_{13i} = \left[0_{2\times m}\right]$$

$$A_{14i} = \begin{bmatrix} \frac{1}{M_i} & \cdots & \frac{1}{M_i} \\ & 0_{1\times n} & \end{bmatrix}, \quad A_{21i} = \left[0_{m\times 2}\right]$$

$$A_{22i} = -A_{23i} = diag\left\{-\frac{1}{T_{t1i}}, \quad \ldots, \quad -\frac{1}{T_{tmi}}\right\}$$

$$A_{24i} = \left[0_{m\times n}\right], A_{31i} = \begin{bmatrix} -\frac{1}{T_{G1i}R_{1i}} & \cdots & -\frac{1}{T_{Gmi}R_{mi}} \\ & 0_{1\times m} & \end{bmatrix}^T$$

$$A_{32i} = \left[0_{m\times m}\right], \; A_{33i} = diag\left\{-\frac{1}{T_{G1i}}, \quad \ldots, \quad -\frac{1}{T_{Gmi}}\right\}$$

$$A_{34i} = \left[0_{n\times m}\right], \; A_{41i} = \begin{bmatrix} -\frac{\rho_1 K_{ev1,i}}{T_{ev1,i}} & \cdots & -\frac{\rho_n K_{evn,i}}{T_{ev1,i}} \\ & 0_{1\times n} & \end{bmatrix}$$

$$A_{42i} = A_{43i} = \left[0_{n\times m}\right]$$

$$A_{44i} = diag\left\{-\frac{1}{T_{ev1,i}}, \quad \ldots, \quad -\frac{1}{T_{evn,i}}\right\}, \; B_i = \begin{bmatrix} 0_{2\times 1} \\ 0_{m\times 1} \\ B_{3i} \end{bmatrix}$$

$$F_i = \begin{bmatrix} -\frac{1}{M_i} \\ 0_{(2m+n+1)\times 1} \end{bmatrix}, \; C_i = \left[\beta_i, \quad 1, \quad 0_{1\times(2m+n)}\right]$$

$$B_{3i} = \left[\frac{\alpha_{1i}}{T_{G1i}}, \ldots, \frac{\alpha_{mi}}{T_{Gmi}}, \frac{\alpha_{(m+1)i} K_{ev1,i}}{T_{ev1,i}}, \ldots, \frac{\alpha_{(m+n)i} K_{evn,i}}{T_{evn,i}}\right]^T$$

According to [25], external disturbances are not taken into consideration when analyzing the internal stability of the system. Such that, by reordering the time-delays in system (4) like:

$$0 = \tau_0 \leqslant \tau_1 \leqslant \ldots \leqslant \tau_N, \tag{5}$$

system (4) can be rewritten as following without external disturbances:

$$\dot{x}(t) = \sum_{i=0}^{N} A_i x(t - \tau_i) \tag{6}$$

where $A_0 = A, A_i = A_{di}$.

III. IMPROVED STABILITY CRITERIA BASED ON B-L INEQUALITY AND MODEL RECONSTRUCTION TECHNIQUE

Two novel stability criteria are proposed in this section based on B-L inequality and model reconstruction technique to obtain more accurate delay margin and to reduce the computational complexity, respectively. The following lemma will be helpful to derive the new criteria.

Lemma 1 [26]: Let $x : [a, b] \to R^n$ be a differentiable function and M be any natural number. For any given matrix $Z\left(\in R^{n\times n}\right) > 0$, the following inequality holds:

$$-\int_\alpha^\beta \dot{x}^T(u) Z \dot{x}(u) \leq -\frac{1}{\beta-\alpha}\zeta_M^T \left[\sum_{k=0}^{M}(2k+1)\varpi_M^T(k) Z \varpi_M(k)\right]\zeta_M \tag{7}$$

where

$$\zeta_M = \begin{cases} [x^T(\beta), x^T(\alpha)]^T, & M = 0, \\ [x^T(\beta), x^T(\alpha), \frac{1}{\beta-\alpha}\Theta_0^T, \ldots, \frac{1}{\beta-\alpha}\Theta_{M-1}^T]^T, & M > 0, \end{cases}$$

$$\varpi_M(k) = \begin{cases} [I, -I], & M = 0, \\ [I, \; (-1)^{k+1} I, \; \theta_{Mk}^0 I, \; \ldots, \; \theta_{Mk}^{M-1} I], & M > 0, \end{cases}$$

$$\theta_{Mk}^j = \begin{cases} (2j+1)\left((-1)^{k+j} - 1\right), & j \leq k, \\ 0, & j > k, \end{cases}$$

$$F_k(u) = (-1)^k \sum_{i=0}^{k} \left[(-1)^i \binom{k}{i}\binom{k+i}{i}\right] \left(\frac{u-\alpha}{u-\beta}\right)^i,$$

$$\Theta_k = \int_\alpha^\beta F_k(u)x(u)du.$$

Remark 2: This inequality is called B-L inequality and the binomial coefficients $\frac{n!}{m!(\text{n-m})!}$ is presented by $\binom{n}{m}$. The right term of the inequality sign is used to estimate the left integral term and with M going to infinity, the right term is approximately equal to the left term. B-L inequality helps a lot to reduce conservativeness in stability analysis of time-delayed systems, but the larger M will bring more complex calculations.

The next stability criterion for system (6) is derived based on Lemma 1 as follows:

Theorem 3: For given scalars τ_i, $i = 0, 1, \ldots, N$, satisfying (5), system (4) is asymptotically stable, if there exist symmetric matrices $P > 0$, $Q_i > 0$, $R_i > 0$, $i = 0, 1, \ldots, N$, such that the following LMI holds:

$$\Phi = \Omega + \Omega^T + \sum_{i=1}^{N} \Psi_i < 0 \tag{8}$$

where

$$\Omega = \begin{bmatrix} e_1 \\ (\tau_1-\tau_0)\, e_{N+2} \\ \vdots \\ (\tau_N-\tau_{N-1})\, e_{2N+1} \\ (\tau_1-\tau_0)\, e_{2N+2} \\ \vdots \\ (\tau_N-\tau_{N-1})\, e_{3N+1} \end{bmatrix}^T P \begin{bmatrix} e_s \\ e_1-e_2 \\ \vdots \\ e_N-e_{N+1} \\ e_1+e_2-2e_{N+2} \\ \vdots \\ e_N+e_{N+1}-2e_{2N+1} \end{bmatrix},$$

$$\Psi_i = e_i^T Q_i e_i - e_{i+1}^T Q_i e_{i+1} + (\tau_i-\tau_{i+1})^2 e_s^T R_i e_s - \begin{bmatrix} e_i-e_{i+1} \\ e_i+e_{i+1}-2e_{N+i+1} \\ e_i-e_{i+1}-6e_{2N+i+1} \end{bmatrix}^T \times \tilde{R}_i \begin{bmatrix} e_i-e_{i+1} \\ e_i+e_{i+1}-2e_{N+i+1} \\ e_i-e_{i+1}-6e_{2N+i+1} \end{bmatrix},$$

$$\tilde{R}_i = diag\left\{R_i, \quad 3R_i, \quad 5R_i\right\}, \; e_s = \sum_{j=0}^{N} A_j e_{j+1},$$

$$e_i = \left[0_{n\times(i-1)n}, \quad I_{n\times n} \quad 0_{n\times(3N+1-i)n}\right], \quad i = 1, 2, \ldots, 3N+1, \; n = N(2m+n+3) - 1.$$

Proof: Choose the following LKF candidate:

$$V(t) = \kappa^T(t) P\kappa(t) + \sum_{i=1}^{N} \int_{t-\tau_i}^{t-\tau_{i-1}} x^T(s) Q_i x(s)\, ds + \sum_{i=1}^{N} (\tau_i-\tau_{i-1})^2 \int_{-\tau_i}^{-\tau_{i-1}} \int_{t+\theta}^{t} \dot{x}^T(s) R_i \dot{x}(s)\, ds d\theta, \tag{9}$$

where

$$\kappa(t) = \begin{bmatrix} x(t) \\ \int_{t-\tau_1}^{t-\tau_0} x(s)\, ds \\ \vdots \\ \int_{t-\tau_N}^{t-\tau_{N-1}} x(s)\, ds \\ \int_{t-\tau_1}^{t-\tau_0} \left(2\frac{s-t+\tau_1}{\tau_1-\tau_0} - 1\right) x(s)\, ds \\ \vdots \\ \int_{t-\tau_N}^{t-\tau_{N-1}} \left(2\frac{s-t+\tau_N}{\tau_N-\tau_{N-1}} - 1\right) x(s)\, ds \end{bmatrix}$$

and then applying Lemma 1 with $M = 2$ to estimate the integral term $-\int_{t-\tau_i}^{t-\tau_{i-1}} \dot{x}^T(s) R_i \dot{x}(s)\, ds$ in the derivative of $V(t)$, yields

$$\dot{V}(t) \le \xi^T(t)\, \Phi \xi(t) \tag{10}$$

where

$$\xi(t) = \begin{bmatrix} x(t-\tau_0) \\ \vdots \\ x(t-\tau_N) \\ \frac{1}{\tau_1-\tau_0}\int_{t-\tau_1}^{t-\tau_0} x(s)\, ds \\ \vdots \\ \frac{1}{\tau_N-\tau_{N-1}}\int_{t-\tau_N}^{t-\tau_{N-1}} x(s)\, ds \\ \frac{1}{\tau_1-\tau_0}\int_{t-\tau_1}^{t-\tau_0} \left(2\frac{s-t+\tau_1}{\tau_1-\tau_0} - 1\right) x(s)\, ds \\ \vdots \\ \frac{1}{\tau_N-\tau_{N-1}}\int_{t-\tau_N}^{t-\tau_{N-1}} \left(2\frac{s-t+\tau_N}{\tau_N-\tau_{N-1}} - 1\right) x(s)\, ds \end{bmatrix}$$

It is obvious that $V(t) > 0$ and $\dot{V}(t) < -\varepsilon \|x(t)\|^2$ for a sufficient small scalar $\varepsilon > 0$, which guarantees the asymptotical stability of system (6) if (8) holds. By employing B-L inequality with $M = 2$, we can reduce the conservativeness to a great extent. The delay margin we can obtain from the LMI toolbox in Matlab software is closer to the true value than Wirtinger inequality [17] and Jensen inequality [16], and this compare will be shown in the next section. However, the use of B-L inequality increases computational complexity and with the increasing of dimensions of system matrices, the increasing of computational complexity will become more obvious. A model reconstruction technique was provided in [17], which helps a lot to reduce the computational complexity. It separates the states in $x(t)$ into n_1 delay-related states and n_2 delay-free states. The n_1 delay-related states and n_2 delay-free states forms $x_1(t)$ and $x_2(t)$ respectively. The smaller n_1 is, the less computational complexity can be obtained. This technique is very suitable for the model of Fig. 1 which also supports us to establish the next stability criterion for system (6).

Theorem 4: For given scalars τ_i, $i = 0, 1, \ldots, N$, satisfying (5), the system (6) is asymptotically stable, if there exist symmetric matrices $P_1 > 0$, $U_i > 0$, $Z_i > 0$, $i = 0, 1, \ldots, N$, such that the following LMI holds:

$$\Xi = \Delta + \Delta^T + \sum_{i=1}^{N} \Upsilon_i < 0 \tag{11}$$

where

$$\Delta = \begin{bmatrix} \bar{e}_1 \\ \bar{e}_0 \\ (\tau_1 - \tau_0)\,\bar{e}_{N+2} \\ \vdots \\ (\tau_N - \tau_{N-1})\,\bar{e}_{2N+1} \\ (\tau_1 - \tau_0)\,\bar{e}_{2N+2} \\ \vdots \\ (\tau_N - \tau_{N-1})\,\bar{e}_{3N+1} \end{bmatrix}^T P_1 \begin{bmatrix} \bar{e}_{s1} \\ \bar{e}_{s0} \\ \bar{e}_1 - \bar{e}_2 \\ \vdots \\ \bar{e}_N - \bar{e}_{N-1} \\ \bar{e}_1 + \bar{e}_2 - 2\bar{e}_{N+2} \\ \vdots \\ \bar{e}_N + \bar{e}_{N+1} - 2\bar{e}_{2N+1} \end{bmatrix}$$

$$\Upsilon_i = \bar{e}_i^T U_i \bar{e}_i - \bar{e}_{i+1}^T U_i \bar{e}_{i+1} + (\tau_i - \tau_{i-1})^2\, \bar{e}_{s1} Z_i \bar{e}_{s1} - \begin{bmatrix} \bar{e}_i - \bar{e}_{i+1} \\ \bar{e}_i + \bar{e}_{i+1} - 2\bar{e}_{N+i+1} \\ \bar{e}_i - \bar{e}_{i+1} - 6\bar{e}_{2N+i+1} \end{bmatrix}^T \tilde{Z}_i \begin{bmatrix} \bar{e}_i - \bar{e}_{i+1} \\ \bar{e}_i + \bar{e}_{i+1} - 2\bar{e}_{N+i+1} \\ \bar{e}_i - \bar{e}_{i+1} - 6\bar{e}_{2N+i+1} \end{bmatrix},$$

$$\tilde{Z}_i = diag\left\{Z_i, \quad 3Z_i, \quad 5Z_i\right\}, \bar{e}_0 = [0_{n_2 \times (3N+1)n_1}, I_{n_2 \times n_2}],$$

$$\bar{e}_1 = [0_{n_1 \times (i-1)n_1}, I_{n_1 \times n_1}, 0_{n_1 \times (3N+1-i)}, 0_{n_1 \times n_2}],$$

$$i = 1,\ 2,\ \ldots,\ 3N+1,$$

$$\bar{e}_{s0} = A_{21}\bar{e}_1 + A_{22}\bar{e}_0 + \sum_{i=1}^{N} A_{di}\bar{e}_{i+1},\ \bar{e}_{s1} = A_{11}\bar{e}_1 + A_{12}\bar{e}_0.$$

Remark 5: Theorem 4 is established based on Lemma 1 ($M = 2$) and model reconstruction technique but the proof of it is omitted here due to the space limitation. It should be noted that separating $x(t)$ into $x_1(t)$ and $x_2(t)$ makes the choice of LFK to prove Theorem 4 different from (9). The dimensions of the positive matrices in Theorem 4 (P_1, U_i, Z_i) are smaller than those in Theorem 3 (P, Q_i, R_i) which make the number of variables that Theorem 4 brings are quite smaller than the one that Theorem 3 brings and the comparison will be given in the next section. At last, [17] gives detailed procedures of how to set $n_1, n_2, A_{11}, A_{12}, A_{21}, A_{22}$ and A_{di} which also helps to prove Theorem 4.

IV. CASE STUDIES

Some case studies are presented in the following subsections including the effectiveness of the proposed method, interaction of time-delays between areas, effect of gains of EVs and the compare between Theorem 3 and Theorem 4. System parameters are given in Tab. 1. Only two areas with 1 governor and turbine and 1 EVs aggregator ($N = 2, m = 1, n = 1$) are considered in order to improve the program running speed in Matlab LMI toolbox.

The whole analysis steps are summarized in [16] which are of great assistance in obtaining the following tables and figures.

TABLE 1. System parameters.

	Areas							
	1	2		1	2		1	2
T_t	0.32	0.30	M	0.1667	0.2084	K_{ev}	1	1
T_G	0.06	0.06	β	0.425	0.397	T_{ev}	0.1	0.1
R	2.4	2.5	ρ	0.417	0.400	α_1	0.5	0.5
D	0.0084	0.0084	T_{12}	0.245		α_2	0.5	0.5

TABLE 2. Delay margins derived by different methods ($K_P = 0.4, K_I = 0.2, K_D = 0$).

	$\tau\,(s)$		
θ	[16]	[17]	Theorem 1
0°	8.38	12.07	12.63
12°	8.51	12.04	13.06
24°	8.46	12.70	14.27
36°	7.98	12.56	14.43
48°	7.72	12.42	12.55
60°	8.28	12.62	15.19
72°	8.57	12.68	13.43
84°	8.46	12.09	12.67

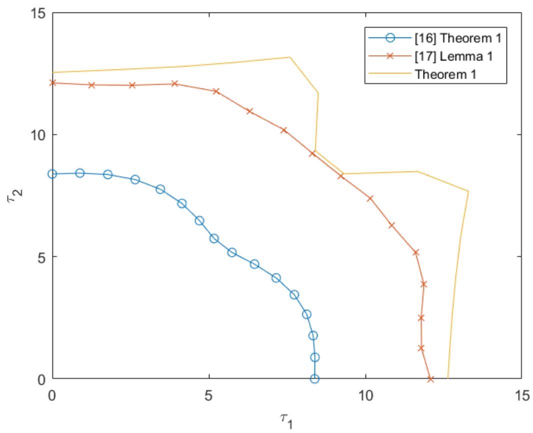

FIGURE 2. Stability regions derived by different methods ($K_P = 0.4, K_I = 0.2, K_D = 0$).

A. EFFECTIVENESS OF THE PROPOSED METHOD

To show the effectiveness of Theorem 3, we compare it with Theorem 1 in [16] and Lemma 1 in [17]. Besides, we use Matlab Simulink to evaluate the frequency deviation of area 1 to verify the accuracy of delay margins obtained by Theorem 3, which is also compared with Lemma 1 in [17].

For the two-area time-delayed LFC system with one governor and turbine and one EVs aggregator, the gains of the PID controllers are set to (0.4, 0.2, 0). The delay margins calculated by Theorem 3, Theorem 1 in [16] and Lemma 1 in [17] are listed in Tab. 2, in which $\tau = \sqrt{\tau_1^2 + \tau_2^2}$ and $\theta = arctan\,(\tau_2/\tau_1)$ [12]. The boundaries of stability regions based on the delay margins are shown in Fig. 2. The time domain response of frequency deviation of area 1 with a step load disturbance appearing at 10s is shown in Fig. 3 where the gains of the PID controllers are set to (0.4, 0.2, 0).

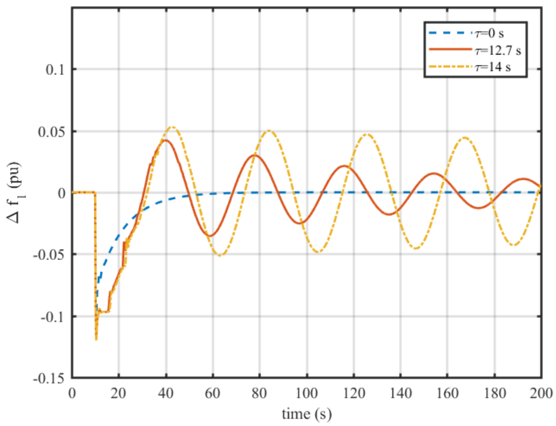

FIGURE 3. Frequency deviation of area 1 with different time-delays($K_P = 0.4, K_I = 0.2, K_D = 0$).

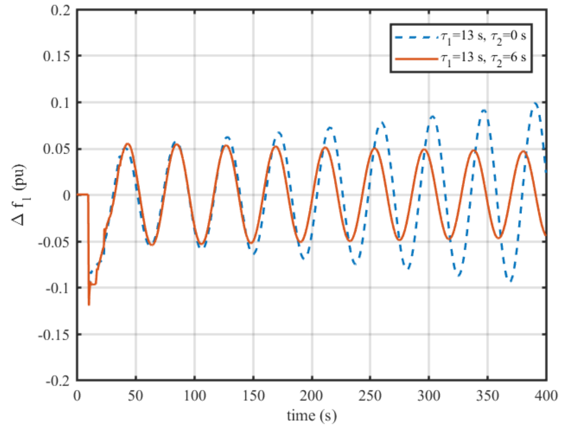

FIGURE 4. Frequency deviation of area 1 with different time-delays ($K_P = 0.2, K_I = 0.2, K_D = 0$).

From the results that shown in the Tab. 2 and Fig. 2, it is easy to find out that the delay margins derived by Theorem 3 are more accurate than which derived by Theorem 1 in [16] and Lemma 1 in [17]. Comparing Theorem 3 with Lemma 1 in [17], the calculation results are very close when θ is around 45°, which means the results calculated by the two methods are both almost the true value of delay margins in this range. To verify the accuracy of delay margins that Theorem 3 brings, frequency deviation of area 1 with τ set to 0s, 12.7s and 14s and θ set to 24° is shown in Fig. 3. $\tau = 12.7s$ is calculated by Lemma 1 in [17] while $\tau = 14$ is calculated by Theorem 3 which can be found in Tab. 2. It is obvious that the frequency deviations are both stable under the time-delays of 12.7s and 14s, but the later one shows less conservative than the former one, which explains the effectiveness of the proposed method.

B. INTERACTION OF TIME-DELAYS BETWEEN AREAS

Sometimes, the increase of time-delay in one area does not decrease the stability region of the other area but increase it slightly. In other words, time-delay will play a positive role in the time-delayed LFC systems with EV aggregators. The simulation verifies this interesting finding.

As is shown in Fig. 4, the time-delay in area 1 is 13s while the time-delays in area 2 are 0s and 6s represented respectively by different lines in the figure. As the time-delay in area 2 rises from $0s$ to $6s$, the performance of frequency deviation of area 1 turns from instable to stable. This is a good example to show that the time-delay in area 2 has a positive impact on area 1. While it is also easy to explain this phenomenon. When $\tau_1 = 13s$ and $\tau_2 = 0s$, τ calculated by $\tau = \sqrt{\tau_1^2 + \tau_2^2}$ is 13s ($\theta = 0°$) and τ now is larger than the delay margin calculated by Theorem 3 (see Tab. 4), which causes instability of frequency deviation of area 1. While $\tau_1 = 13s$ and $\tau_2 = 6s$, τ is calculated equaling to 14.3s and θ approximately equals to 60°, and the delay margin can be found in Tab. 4 is $14.7s$ which is larger than τ, thus the frequency deviation of area 1 is stable. Hence one can see that the interaction of time-delays between areas in the time-delayed multi-area LFC system with EV aggregators.

TABLE 3. Delay margins with different K_{ev}s ($K_P = 0.15, K_I = 0.2, K_D = 0.05$).

	$\tau(s)$		
θ	$K_{ev,i} = 1$	$K_{ev,i} = 0.7$	$K_{ev,i} = 0.3$
0°	11.93	13.95	18.08
15°	12.54	14.68	19.05
30°	13.48	15.82	19.98
45°	11.50	13.50	17.48
60°	13.43	15.75	19.98
75°	12.45	14.57	18.93
90°	11.84	13.85	17.97

C. EFFECT OF GAINS OF EVs

The battery's state of charge (SOC) is an important feature of EVs which affects the gains of EVs. Many papers do not take SOC into consideration and only set $K_{ev} = 1$, which are not in conformity with the actual situation. Reference [16] gives a relationship between SOC and K_{ev} described by:

$$K_{ev} = K - Kg(t) \tag{12}$$

where $K = 1$, $g(t) = \left(\frac{SOC_{current} - SOC_{low(high)}}{SOC_{max(min)} - SOC_{low(high)}}\right)^v$.

And the range of $g(t)$ is [0, 1], such that K_{ev} varies from 0 to 1. In other words, K_{ev} is a time-varying parameter which depends on SOC of EVs. K_{ev} is an important factor affecting the delay margin of the time-delayed LFC systems with EV aggregators. Datas in Tab. 3 and Fig. 5 derived by Theorem 3 both confirm this finding.

No matter how the gains of the PID controllers change, the stability region of the time-delayed two-area LFC systems with EV aggregators decreases with the increase of K_{ev}s, which means the higher the current SOC is, the larger the stability region can be obtained.

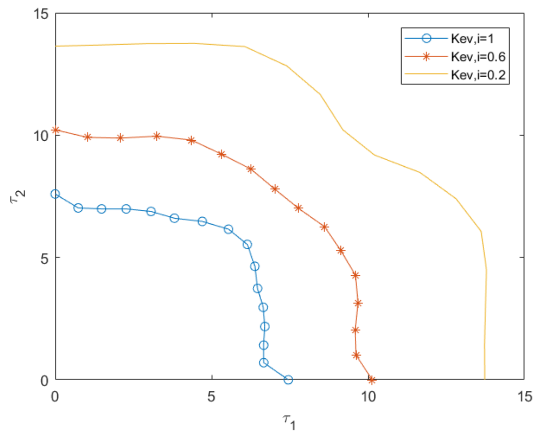

FIGURE 5. Stability regions with different K_{ev}s ($K_P = 0.5, K_I = 0.3, K_D = 0.1$).

TABLE 4. Delay margins derived by Theorem 3 and Theorem 4 ($K_P = 0.2, K_I = 0.2, K_D = 0$).

	$\tau\,(s)$	
θ	Theorem 1	Theorem 2
0°	12.09	12.09
12°	12.53	12.53
30°	14.89	14.87
42°	11.92	11.92
60°	14.70	14.68
72°	12.89	12.89
90°	12.00	12.00

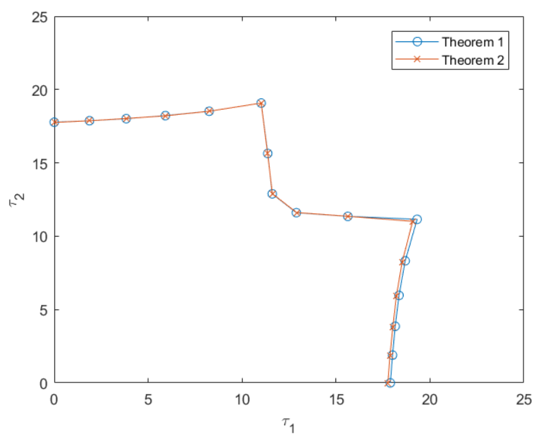

FIGURE 6. Stability regions derived by Theorem 3 and Theorem 4 ($K_P = 0.1, K_I = 0.2, K_D = 0$).

D. COMPARISON BETWEEN THEOREM 1 AND THEOREM 2

Tab. 4 and Fig. 6 show the delay margins and stability regions derived by the two proposed theorems, respectively. The results derived by the two theorems are very close, but Theorem 3 brings 1804 variables while Theorem 4 brings only 556 variables. Thus, the computation speed improves greatly by means of the model reconstruction technique.

Theorem 4 based on model reconstruction technique can reduce the computational complexity without reducing conservativeness when PID gains are set to $(0.2, 0.2, 0)$ or $(0.1, 0.2, 0)$. However, the change of gains of the PID controllers may increase the computational complexity. For example, when K_D is not set to 0, the number of n_1 will increase that will bring more variables. Furthermore, results derived by Theorem 4 are not as accurate as Theorem 3 for some PID gains(see [17] Fig. 2 and Fig. 5). But in general, model reconstruction technique is very effective to the LFC systems with EV aggregators due to the high dimensions of system matrices.

V. CONCLUSION

This paper has investigated the problem of load frequency stability of time-delayed power systems with EV aggregators. A dynamic model of time-delayed LFC system with EV aggregators is presented. Two improved delay-dependent stability criteria have been proposed based on B-L inequality and model reconstruction technique, respectively. The delay margins of the considered systems have been calculated by Matlab/LMI toolbox. Several case studies are used to show the effectiveness of the proposed methods, interaction of time-delays between areas, how gains of EVs affect the delay margins. In addition, some simulations have been presented to verify the obtained results.

REFERENCES

[1] X. Liu, X. Kong, and K. Y. Lee, "Distributed model predictive control for load frequency control with dynamic fuzzy valve position modelling for hydro-thermal power system," *IET Control Theory Appl.*, vol. 10, no. 14, pp. 1653–1664, Sep. 2016.
[2] H. Shayeghi, H. A. Shayanfar, and A. Jalili, "Load frequency control strategies: A state-of-the-art survey for the researcher," *Energy Convers. Manage.*, vol. 50, no. 2, pp. 344–353, Feb. 2009.
[3] M. Yilmaz and P. T. Krein, "Review of the impact of vehicle-to-grid technologies on distribution systems and utility interfaces," *IEEE Trans. Power Electron.*, vol. 28, no. 12, pp. 5673–5689, Dec. 2013.
[4] K. S. Ko, S. Han, and D. K. Sung, "A new mileage payment for EV aggregators with varying delays in frequency regulation service," *IEEE Trans. Smart Grid*, vol. 9, no. 4, pp. 2616–2624, Jul. 2018.
[5] T. N. Pham, H. Trinh, and L. V. Hien, "Load frequency control of power systems with electric vehicles and diverse transmission links using distributed functional observers," *IEEE Trans. Smart Grid*, vol. 7, no. 1, pp. 238–252, Jan. 2016.
[6] H. Bevrani and T. Hiyama, "On load-frequency regulation with time delays: Design and real-time implementation," *IEEE Trans. Energy Convers.*, vol. 24, no. 1, pp. 292–300, Mar. 2009.
[7] X. Yu and K. Tomsovic, "Application of linear matrix inequalities for load frequency control with communication delays," *IEEE Trans. Power Syst.*, vol. 19, no. 3, pp. 1508–1515, Aug. 2004.
[8] K. Liu, A. Selivanov, and E. Fridman, "Survey on time-delay approach to networked control," *Annu. Rev. Control*, vol. 48, pp. 57–79, Jul. 2019.
[9] K. Liu, A. Seuret, Y. Xia, F. Gouaisbaut, and Y. Ariba, "Bessel–Laguerre inequality and its application to systems with infinite distributed delays," *Automatica*, vol. 109, Nov. 2019, Art. no. 108562.
[10] C.-K. Zhang, F. Long, Y. He, W. Yao, L. Jiang, and M. Wu, "A relaxed quadratic function negative-determination lemma and its application to time-delay systems," *Automatica*, vol. 113, Mar. 2020, Art. no. 108764.
[11] C.-K. Zhang, Y. He, L. Jiang, M. Wu, and H.-B. Zeng, "Delay-variation-dependent stability of delayed discrete-time systems," *IEEE Trans. Autom. Control*, vol. 61, no. 9, pp. 2663–2669, Sep. 2016.
[12] H.-B. Zeng, Z.-L. Zhai, Y. He, K.-L. Teo, and W. Wang, "New insights on stability of sampled-data systems with time-delay," *Appl. Math. Comput.*, vol. 374, Jun. 2020, Art. no. 125041.

[13] A. Seuret and F. Gouaisbaut, "Wirtinger-based integral inequality: Application to time-delay systems," *Automatica*, vol. 49, no. 9, pp. 2860–2866, 2013.
[14] H.-B. Zeng, Y. He, M. Wu, and J. She, "Free-matrix-based integral inequality for stability analysis of systems with time-varying delay," *IEEE Trans. Autom Control.*, vol. 60, no. 10, pp. 2768–2772, Oct. 2015.
[15] H.-B. Zeng, X.-G. Liu, and W. Wang, "A generalized free-matrix-based integral inequality for stability analysis of time-varying delay systems," *Appl. Math. Comput.*, vol. 354, pp. 1–8, Aug. 2019.
[16] C.-K. Zhang, L. Jiang, Q. H. Wu, Y. He, and M. Wu, "Further results on delay-dependent stability of multi-area load frequency control," *IEEE Trans. Power Syst.*, vol. 28, no. 4, pp. 4465–4474, Nov. 2013.
[17] L. Jin, C.-K. Zhang, Y. He, L. Jiang, and M. Wu, "Delay-dependent stability analysis of multi-area load frequency control with enhanced accuracy and computation efficiency," *IEEE Trans. Power Syst.*, vol. 34, no. 5, pp. 3687–3696, Sep. 2019.
[18] F. Yang, J. He, J. Wang, and M. Wang, "Auxiliary-function-based double integral inequality approach to stability analysis of load frequency control systems with interval time-varying delay," *IET Control Theory Appl.*, vol. 12, no. 5, pp. 601–612, Mar. 2018.
[19] L. Xiong, H. Li, and J. Wang, "LMI based robust load frequency control for time delayed power system via delay margin estimation," *Int. J. Elect. Power Energy Syst.*, vol. 100, pp. 91–103, Sep. 2018.
[20] K. S. Ko and D. K. Sung, "The effect of EV aggregators with time-varying delays on the stability of a load frequency control system," *IEEE Trans. Power Syst.*, vol. 33, no. 1, pp. 669–680, Jan. 2018.
[21] T. N. Pham, S. Nahavandi, L. V. Hien, H. Trinh, and K. P. Wong, "Static output feedback frequency stabilization of time-delay power systems with coordinated electric vehicles state of charge control," *IEEE Trans. Power Syst.*, vol. 32, no. 5, pp. 3862–3874, Sep. 2017.
[22] T. N. Pham, H. Trinh, and A. M. T. Oo, "Distributed control of HVDC links for primary frequency control of time-delay power systems," *IEEE Trans. Power Syst.*, vol. 34, no. 2, pp. 1301–1314, Mar. 2019.
[23] H. Fan, L. Jiang, C.-K. Zhang, and C. Mao, "Frequency regulation of multi-area power systems with plug-in electric vehicles considering communication delays," *IET Gener., Transmiss. Distrib.*, vol. 10, no. 14, pp. 3481–3491, Nov. 2016.
[24] F. Yang, J. He, and Q. Pan, "Further improvement on delay-dependent load frequency control of power systems via truncated B-L inequality," *IEEE Trans. Power Syst.*, vol. 33, no. 5, pp. 5062–5071, Sep. 2018.
[25] W. Tan, H. Zhang, and M. Yu, "Decentralized load frequency control in deregulated environments," *Int. J. Elect. Power Energy Syst.*, vol. 41, no. 1, pp. 16–26, Oct. 2012.
[26] A. Seuret and F. Gouaisbaut, "Hierarchy of LMI conditions for the stability analysis of time-delay systems," *Syst. Control Lett.*, vol. 81, no. 1, pp. 1–7, Jul. 2015.

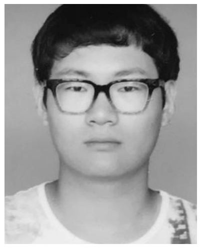

SHA-JUN ZHOU was born in Nantong, Jiangsu, China, in 1996. He received the B.S. degree in electronic engineering from the Hunan University of Technology, Zhuzhou, China, in 2018, where he is currently pursuing the M.S. degree. His research interest is time-delay system and its applications.

HONG-BING ZENG received the B.Sc. degree in electrical engineering from the Tianjin University of Technology and Education, Tianjin, China, in 2003, the M.Sc. degree in computer science from the Central South University of Forestry, Changsha, China, in 2006, and the Ph.D. degree in control science and engineering from Central South University, Changsha, in 2012. From 2013 to 2014, he was a Postdoctoral Research Associate with the Department of Electrical Engineering, Yeungnam University, Kyongsan, South Korea. Since 2003, he has been with the Department of Electrical and Information Engineering, Hunan University of Technology, Zhuzhou, China, where he is currently a Professor of automatic control engineering. His current research interests are time-delay systems, neural networks, and networked control systems.

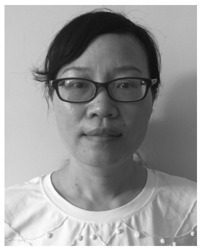

HUI-QIN XIAO received the B.Sc. degree majoring in automation from the Hunan University of Technology, China, in 2000, and the M.Sc. degree in control theory and control engineering and the Ph.D. degree in control science and engineering from Central South University, Changsha, China, in 2006 and 2015, respectively. Since 2000, she has been with the Department of Electrical and Information Engineering, Hunan University of Technology, Zhuzhou, China, where she is currently an Associate Professor of automatic control engineering. Her current research interests are time-delay systems, nonlinear control systems, and networked control systems.